

# Recent CMB Observations and the Ionization History of the Universe

Steen Hannestad<sup>1</sup> and Robert J. Scherrer<sup>2,3</sup>

<sup>1</sup>*NORDITA, Blegdamsvej 17, DK-2100 Copenhagen, Denmark*

<sup>2</sup>*Department of Physics, The Ohio State University, Columbus, OH 43210*

<sup>3</sup>*Department of Astronomy, The Ohio State University, Columbus, OH 43210*

(December 24, 2018)

Recent cosmic microwave background (CMB) results from BOOMERANG and MAXIMA show an unexpectedly low second acoustic peak, resulting in a best-fit baryon density that is 50% larger than the prediction of big-bang nucleosynthesis (BBN). This problem can be avoided if the universe has a non-standard ionization history where the recombination of hydrogen is significantly delayed relative to the standard model. We examine non-standard models in which the hydrogen binding energy  $E_b$  and the overall expression for the time rate of change of the ionized fraction of electrons are multiplied by arbitrary factors. This set of models includes a number of previously-proposed models as special cases. We find a wide range of models with delayed recombination that are able to fit the CMB data with a baryon density in accordance with BBN, but there are even allowed models with *earlier* recombination than in the standard model. A generic prediction of our model is that the third acoustic CMB peak should be very low relative to what is found in the standard model. This is the case even for the models with earlier recombination than in the standard model, because here the third peak is lowered by an increased diffusion damping at recombination relative to the standard model. Interestingly, the specific height of the third peak depends sensitively on the model parameters, so that future CMB measurements will be able to distinguish between different non-standard recombination scenarios.

## I. INTRODUCTION

In the past year, observations of the cosmic microwave background (CMB) fluctuations by the BOOMERANG [1] and MAXIMA [2] experiments have produced data of unprecedented precision on CMB fluctuations at small angular scales. While generally confirming the adiabatic, flat ( $\Omega \approx 1$ ) model predicted by inflation, these observations have several puzzling features. In particular, the position of the first acoustic peak is at a slightly larger angular scale than is predicted in the flat model, and the amplitude of the second peak is unexpectedly low (see, e.g., Ref. [3]). If these results are fit using the standard set of cosmological parameters, the result is a CMB prediction for the baryon density of  $\Omega_b h^2 \sim 0.03$  [4] - [6]. In contrast, the prediction for  $\Omega_b h^2$  from Big-Bang nucleosynthesis is  $\Omega_b h^2 \sim 0.02$  [7,8].

One way to explain the CMB observations and preserve agreement with the BBN baryon density is to postulate that the epoch of recombination was delayed to a lower redshift than in the standard model. Peebles, Seager, and Hu suggested that this could occur if there were sources of Ly  $\alpha$  photons present at the epoch of recombination [9]. A more speculative mechanism is a time-variation in the fine-structure constant,  $\alpha$  [10]- [15]. The authors of Ref. [15] used such a time-variation (along with changes in the cosmological parameters) as an example of how one might model non-standard recombination in general. Here, we investigate more generic variations in the ionization history.

Ideally, one would like to investigate the consequences for the CMB of an arbitrary  $x_e(z)$ , the ionization fraction as a function of redshift. It is obviously impractical to investigate arbitrary functional forms for  $x_e$ . Instead, we have attempted to parametrize deviations of  $x_e(z)$  from the standard ionization history in terms of a small number of physically-motivated parameters. In particular, we multiply the overall ionization/recombination rates by a free parameter  $a$ , and the binding energies by a parameter  $b$ . We then calculate the predictions for the CMB fluctuation spectrum as a function of these parameters and compare with observations. Our parametrization is discussed in the next section, along with the results of modifying the ionization history. Our conclusions are given in Sec. 3.

## II. NON-STANDARD RECOMBINATION

Given that one cannot examine all possible recombination histories, what is the best subset to investigate? We have attempted to model a subset of such recombination histories which is physically motivated and, at least to some extent, reduces to the Peebles et al. model [9] and the time-varying  $\alpha$  model [10]- [15] as special cases. There are two possible approaches to modifying the ionization history  $x_e(z)$ . We can directly modify this ionization history,

or we can alter the evolution equation for  $dx_e/dt$ . We use the latter approach, but we also examine the relationship between variations in  $dx_e/dt$  and the resulting form for  $x_e(z)$ .

Consider first the equation for  $dx_e/dt$ : [16]- [17]:

$$-\frac{dx_e}{dt} = \mathcal{C} \left[ \mathcal{R} n_p x_e^2 - \beta(1 - x_e) \exp \left( -\frac{B_1 - B_2}{kT} \right) \right], \quad (1)$$

where  $\mathcal{R}$  is the recombination coefficient,  $\beta$  is the ionization coefficient,  $B_n$  is the binding energy of the  $n^{\text{th}}$  H-atom level and  $n_p$  is the sum of free protons and H-atoms. The Peebles correction factor ( $\mathcal{C}$ ) accounts for the effect of the presence of non-thermal Lyman- $\alpha$  resonance photons; it is defined as

$$\mathcal{C} = \frac{1 + A}{1 + A + C} = \frac{1 + K\Lambda(1 - x_e)}{1 + K(\Lambda + \beta)(1 - x_e)}. \quad (2)$$

In the above,  $K = H^{-1} n_p c^3 / 8\pi \nu_{12}^3$  (where  $\nu_{12}$  is the Lyman- $\alpha$  transition frequency), and  $\Lambda$  is the rate of decay of the 2s excited state to the ground state via 2 photons [18]. The ratio  $\beta/\mathcal{R}$  is fixed by detailed balance.

We modify the evolution history for  $x_e$  as follows. We introduce two new parameters,  $a$ , and  $b$ , into equation (1). The parameter  $a$  multiplies the overall rate for  $dx_e/dt$ , while  $b$  multiplies all of the binding energies  $B_n$ . Then equation (1) becomes:

$$-\frac{dx_e}{dt} = a\mathcal{C} \left[ \mathcal{R} n_p x_e^2 - \beta(1 - x_e) \exp \left( -b\frac{B_1 - B_2}{kT} \right) \right]. \quad (3)$$

We take  $a$  and  $b$  to be constants independent of  $z$  (a model with redshift-dependent  $a$  and  $b$  would simply take us back to arbitrary functional behavior for  $x_e(z)$ ). The case  $a = b = 1$  corresponds to the standard model. In order to be completely self-consistent the recombination rate for helium should also be changed with varying  $a$  and  $b$ . However, this is a very small effect and in all our calculations the recombination history of helium is assumed to follow the standard model. This assumption has no bearing on any of our conclusions.

Our  $a$  and  $b$  parameters have a simple physical interpretation. A change in  $a$  alone represents a change in the ionization and recombination rates which preserves detailed balance at a fixed binding energy, since the ratio of the ionization to recombination rate is unchanged. A change in  $b$  alone simply shifts the epoch of recombination up or down in redshift by a fixed amount.

This particular parametrization has several advantages. The time-varying  $\alpha$  model is basically a special case of this model [10,11]. In the Peebles et al. model [9] delayed recombination arises from additional Ly- $\alpha$  resonance photons produced by some unknown source. We have not directly tested this specific model in  $(a,b)$ -space, but instead we have examined a related model in which the rates for the Ly- $\alpha$  and  $2s \rightarrow 1s$  transitions to the ground state are reduced by a factor  $\epsilon$  which is assumed to be constant in time. In this model the Peebles correction factor is changed relative to Eq. (2)

$$\mathcal{C} = \frac{1 + K\Lambda(1 - x_e)}{1 + K(\Lambda + \beta/\epsilon)(1 - x_e)}. \quad (4)$$

Although this model is very similar in behaviour to that of the Peebles et al. model [9], they are not completely equivalent. However, the exact form of the Peebles et al. model is quite speculative, and our purpose here has just been to test some of the possible ways to alter recombination. The Peebles et al. model could be mimicked almost exactly by a time-dependent  $\epsilon$ , but this is an unnecessary complication.

In order to examine the viable region in  $(a,b)$  parameter space we have performed a  $\chi^2$  analysis on the data from the BOOMERANG [1] and MAXIMA [2] experiments. Our procedure is to maximize the likelihood for each point in  $(a,b)$  space for the following free parameters: the total matter density,  $\Omega_m$ , the Hubble parameter,  $H_0$ , the spectral index of the primordial power spectrum,  $n_s$ , and the overall normalization of the spectrum,  $Q$ . We have assumed a flat geometry so that  $\Omega_\Lambda = 1 - \Omega_m$ , and also that reionization is unimportant (assuming that the optical depth to reionization is small,  $\tau \simeq 0$ ). The vector of free parameters is then

$$\theta = \{\Omega_m, H_0, n_s, Q\}, \quad (5)$$

and the likelihood function to be optimized is

$$\mathcal{L} \propto A \exp \left( -\frac{(C_l(\theta) - C_{l,obs})^2}{\sigma^2(C_l)} \right). \quad (6)$$

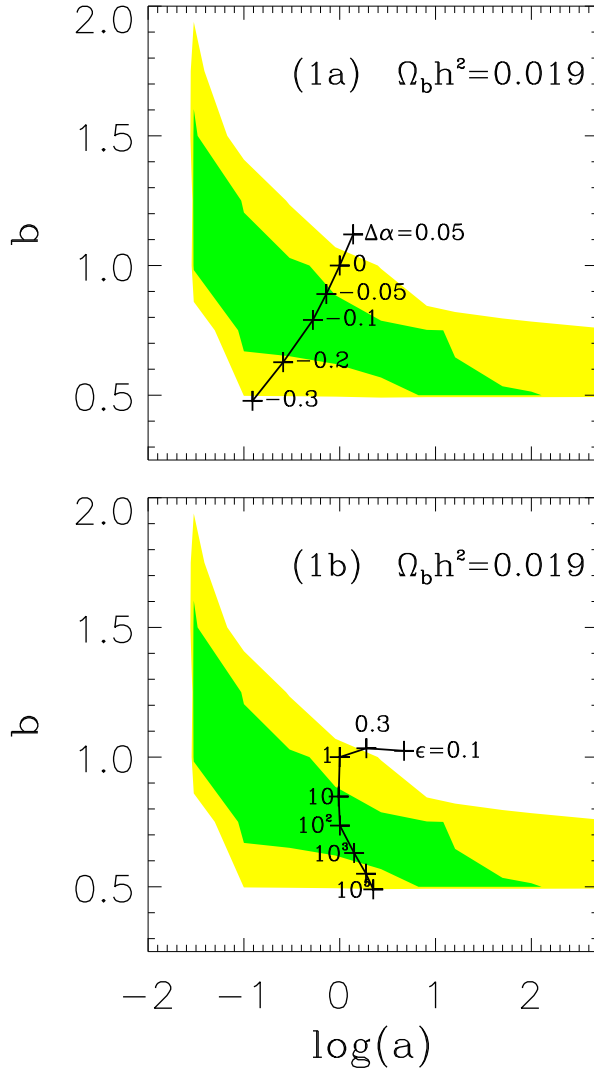


FIG. 1. The allowed region in  $a, b$  parameter space from the combined BOOMERANG and MAXIMA data, assuming a baryon density of  $\Omega_b h^2 = 0.019$ . The dark shaded (green) region is the  $1\sigma$  allowed region, and the light shaded (yellow) is the  $2\sigma$  region. Also shown: 1a) The curve in  $a, b$  space which best fits the varying fine-structure constant ( $\alpha$ ) model for non-standard recombination;  $\Delta\alpha$  is defined as  $\Delta\alpha \equiv (\alpha - \alpha_0)/\alpha_0$ , 1b) The curve which best fits the modified Peebles et al. model for delayed recombination. The quantity  $\epsilon$  is defined in Eq. (4).

The agreement between our models and the observations, as a function of  $a$  and  $b$ , is shown in Figs. 1a and 1b, for  $\Omega_b h^2 = 0.019$ , and in Fig. 2 for  $\Omega_b h^2 = 0.03$ . In both figures, the area outside the dark (green) shaded region is excluded at the  $1 - \sigma$  level, and the area outside the light (yellow) shaded region is excluded at the  $2 - \sigma$  level. The allowed region is a broad band, in which larger values of  $a$  are compensated by smaller values of  $b$ . (Note that the apparent cutoffs at small  $a$  and small  $b$  in Fig. 1 are the real boundaries of the confidence region). This result hides a great deal of information: from these graphs alone it is impossible to tell whether the allowed region corresponds to identical forms for  $x_e(z)$  produced by different values of  $a, b$ , or whether  $x_e(z)$  varies greatly within the allowed region. The latter is, in fact, the case. This is shown in Fig. 3, in which we graph the ionization history for three pairs of  $a, b$  within the allowed region. Increasing  $b$  and decreasing  $a$  results in a surface of last scattering at higher redshift which is much broader.

We also display, for comparison, the values of  $a$  and  $b$  which best fit the models with a change in  $\alpha$  (Fig. 1a) and our version of the Peebles et al. model, given by equation (4) (Fig. 1b). The behavior of the time-varying  $\alpha$  model is easy to understand; an increase in  $\alpha$  results in an increase in all of the binding energies (and thus, an increase in  $b$ ) and it also increases the ionization and recombination rates (an increase in  $a$ ) [10,11]. Thus, the curve corresponding to time-varying  $\alpha$  runs almost perpendicular to our best-fit contour, and we find good agreement for negative values

of  $\Delta\alpha$ , as in Refs. [13] - [15]. In Fig. 1b, we see that the correspondence between the modified Peebles, et al., model and our  $a, b$  formalism is more complicated. The part of the curve corresponding to  $\epsilon < 1$  corresponds to faster than normal recombination and is not physically related to the Peebles et al. model. For  $\epsilon > 1$  both  $a$  and  $b$  are changing with changing  $\epsilon$ . From Fig. 1 in Ref. [9], it is possible to understand the path taken by the curve in  $a, b$ -space. As  $\epsilon$  is increased recombination is pushed to smaller  $z$ , but at the same time the width of the recombination surface decreases. Therefore, for increasing  $\epsilon$ , the best-fit curve should move down and to the right in  $a, b$  space, exactly what is seen from Fig. 1b. This is different from the varying  $\alpha$  curve, where the width of the recombination surface increases as  $\alpha$  decreases. This means that the best-fit values in the time-varying  $\alpha$  model and the best-fit values in the modified Peebles model lie in slightly different parts of the  $a, b$  plane.

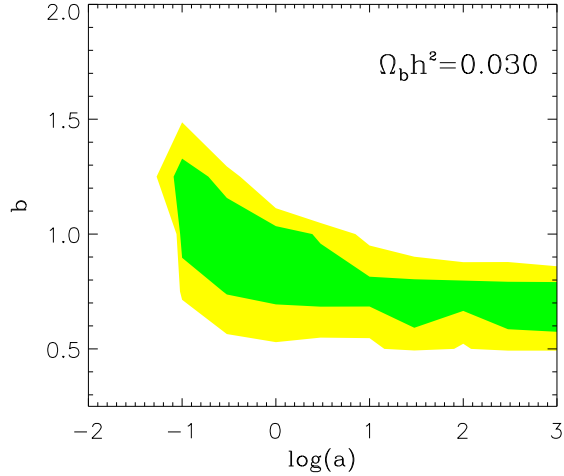


FIG. 2. The light (yellow) and dark (green) shaded regions are equivalent to those in Fig. 1, except that they are calculated assuming a high baryon density,  $\Omega_b h^2 = 0.030$ .

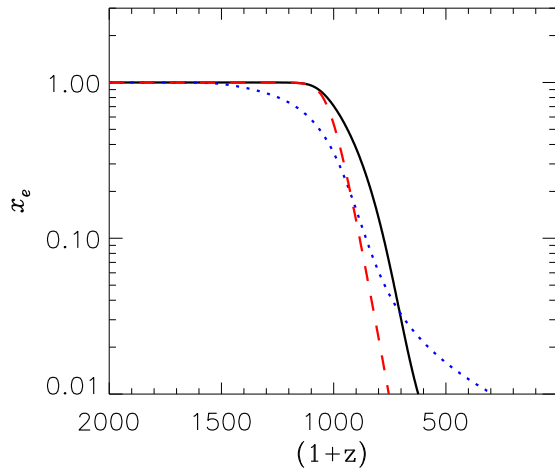


FIG. 3. Three different ionization histories, all chosen to lie within the allowed region. The dotted curve is for  $a = 0.1, b = 1.0$ , the solid curve for  $a = 1.0, b = 0.75$  and the dashed for  $a = 10.0, b = 0.65$ .

On first sight the results in Fig. 3 would mean that the large allowed region in  $(a, b)$ -space is entirely due to degeneracy between  $a, b$  and the other cosmological parameters. In order to investigate this possibility we have

performed a simple Fisher matrix analysis of how degenerate  $a$  and  $b$  are with the other cosmological parameters. The Fisher information matrix is given by [12]

$$F_{ij} = \sum_{l=2}^{l_{\max}} \frac{1}{\sigma(C_l)^2} \frac{\partial C_l}{\partial \theta_i} \frac{\partial C_l}{\partial \theta_j}, \quad (7)$$

where  $i$  and  $j$  denote elements in the vector of cosmological parameters to be determined and  $\sigma(C_l)$  is the uncertainty in the measurement of  $C_l$ . The standard deviation in a measurement of parameter  $\theta_i$  is then given by  $\sigma(\theta_i)^2 = (F^{-1})_{ii}$ . For simplicity we assume that the measurement error in the  $C_l$ 's is purely due to cosmic variance so that

$$\frac{\sigma(C_l)}{C_l} = \sqrt{\frac{2}{2l+1}}. \quad (8)$$

The outcome of this analysis is shown in Figs. 4a and 4b. The precision with which either  $a$  or  $b$  can be determined drops considerably if  $a$  and  $b$  must be determined simultaneously, meaning that  $a$  and  $b$  are to some extent degenerate. However, the biggest loss of precision still comes when the other cosmological parameters have to be determined as well. The partial degeneracy between  $a$  and  $b$  has a simple physical explanation. If the redshift of recombination is lowered the radiation content at recombination is lower, leading to a smaller early ISW effect. On the other hand, if the width of the recombination surface is narrowed, the diffusion damping of fluctuations is smaller. These two effects can to some extent compensate each other, and lead to a partial degeneracy between  $a$  and  $b$ . However, the degeneracy is not exact, because the early ISW effect dominates near the first peak in the spectrum, while the diffusion damping dominates at larger  $l$ .

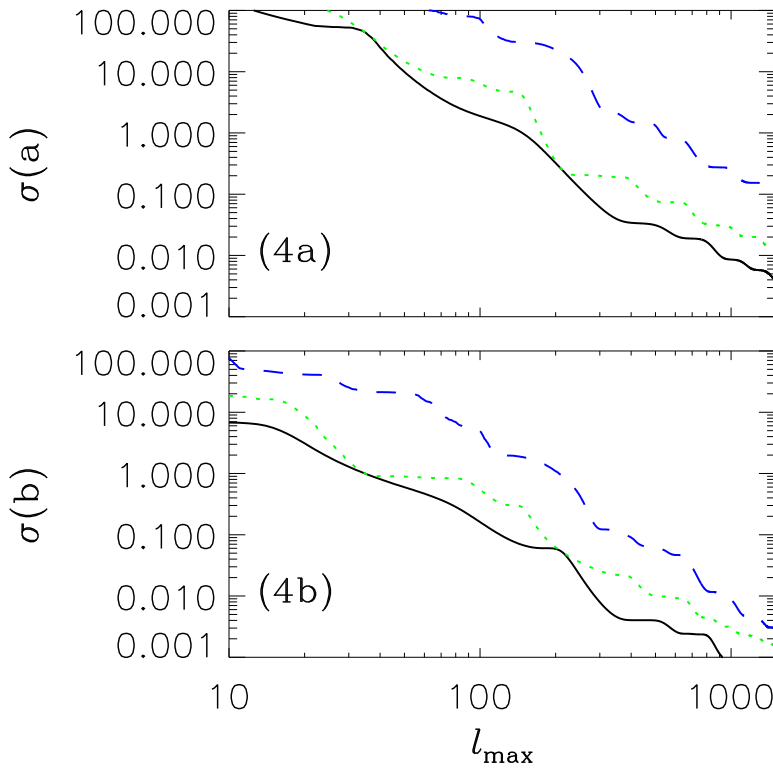


FIG. 4. The expected accuracy with which  $a$  can be measured, as a function of the maximum  $l$  that the power spectrum can be measured to. We have assumed that the power spectrum can be measured at all  $l$ , up to  $l_{\max}$ , to within cosmic variance  $\sigma(C_l)/C_l = [2/(2l+1)]^{1/2}$ . Fig. 4a) The solid line is the expected precision if  $a$  alone needs to be determined from the CMB, the dotted is the case where  $a$  and  $b$  must be simultaneously determined, and the dashed the case where all parameters  $(\Omega_m, \Omega_b, H_0, n_s, Q, a, b)$  must be determined. Fig. 4b) The same as for Fig. 4a, except that  $a$  and  $b$  are interchanged.

A second possible approach to the problem of the CMB as a function of a generic recombination history would be to modify  $x_e(z)$  directly by hand. This is a somewhat unphysical approach, so we have instead examined the general behavior of  $x_e(z)$  as a function of  $a$  and  $b$ . The two key properties of the ionization history which affect the CMB are the redshift of last-scattering, and the width of the last-scattering surface. We parametrize the former in terms of  $z_{1/2}$ , the redshift at which  $x_e = 0.5$ . To estimate the width of the last scattering surface, we define the parameter  $\Delta z$  to be  $z(x_e = 0.9) - z(x_e = 0.1)$ . While both of these definitions are somewhat arbitrary, they serve the desired purpose of indicating the redshift and width of the last scattering surface. The behavior of these quantities as a function of  $a$  and  $b$  is illustrated in Figs. 5 and 6, and in Fig. 7 we show  $\Delta z/z_{1/2}$  as a function of  $a$  and  $b$ .

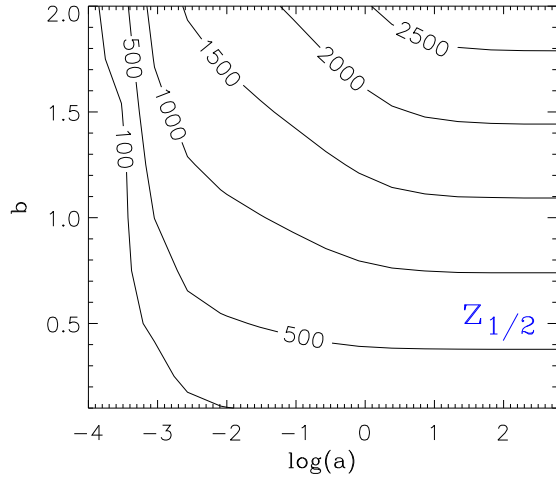


FIG. 5. The redshift of last scattering ( $z_{1/2}$ ) as a function of  $a$  and  $b$ .

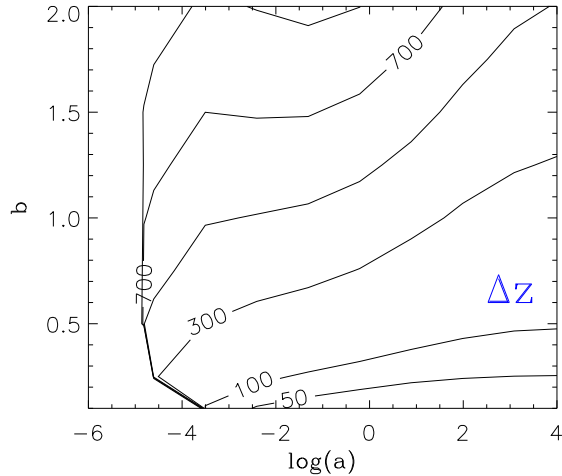


FIG. 6. The width of the last scattering surface ( $\Delta z$ ) as a function of  $a$  and  $b$ .

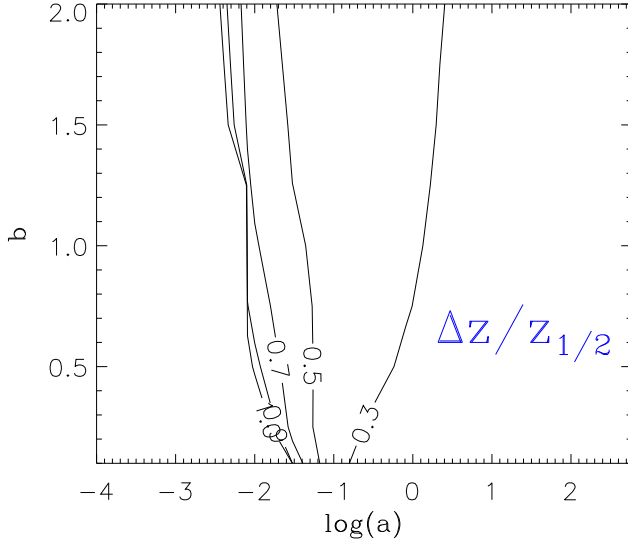


FIG. 7. The width of the last scattering surface relative to the redshift of last scattering,  $\Delta z/z_{1/2}$ , as a function of  $a$  and  $b$ .

Several features are obvious from these plots. In Fig. 5, we see that  $z_{1/2}$  is a function only of  $b$  (and is independent of  $a$ ) in the limit where  $a > 1$ . This result follows from the fact that for large  $a$ , the ionization fraction tracks its equilibrium value nearly exactly, and the equilibrium value of  $x_e$  at fixed  $z$  depends only on the binding energies (and hence, on  $b$ ). This argument breaks down for small  $a$ , since in this case the ionization fraction no longer tracks the equilibrium abundance. In the limit of extremely small  $a$ , recombination is continuing at the present, and the lower limit  $x_e = 0.1$  we use to calculate  $\Delta z$  is never reached. Hence, there is a limiting value for  $a$  below which  $\Delta z$  is undefined; this is reflected in the degeneracy of our contours for small  $a$  in Fig. 6. If we define the width of our last scattering surface relative to the redshift of last scattering (as in Fig. 7), then we see that  $\Delta z/z_{1/2}$  is essentially a function of  $a$ , and is nearly independent of  $b$ . At large  $a$ , the ionization fraction tracks its equilibrium value nearly exactly (and so is independent of  $a$ ). Furthermore, when  $x_e(z)$  is given by the Saha equation,  $\Delta z/z_{1/2}$  is independent of the binding energy. Thus  $\Delta z/z_{1/2}$  becomes independent of both  $a$  and  $b$  for large values of  $a$ , as seen in Fig. 7.

Figs. 5 and 6 indicate that scanning over all possible values of  $a$  and  $b$  is nearly equivalent to scanning over all possible values of the redshift and width of the last scattering surface. Hence, our method of varying  $a$  and  $b$  provides a quite general study of arbitrary ionization histories. The one exception is the case of large  $z_{1/2}$  and small  $\Delta z$ , which does not correspond to any values of  $a$  and  $b$ . However, this case corresponds to a decrease in  $x_e$  which occurs faster than for the equilibrium case. It is difficult to imagine a mechanism for achieving this. Furthermore, we expect the  $C_l$  spectrum to become independent of  $\Delta z$  for sufficiently small  $\Delta z$ , since the thickness of the last-scattering surface will become irrelevant when it becomes so narrow that diffusion damping can be neglected. For completeness we have also calculated  $\chi^2$  for the case of  $\Delta z = 0$ , for which we take  $x_e$  to be a step function. These are shown in Fig. 8. We see that no good fit is obtained for any value of  $z_{1/2}$  ( $\chi^2_{\min}/\text{d.o.f} \simeq 3.8$ ).

If we consider the allowed region in Fig. 1 as a function of  $z_{1/2}$  and  $\Delta z$ , rather than  $a$ , and  $b$ , we find that both  $\Delta z$  and  $z_{1/2}$  are restricted by the current CMB observations. At the 95% confidence level, we have  $300 < \Delta z < 900$  and  $500 < z_{1/2} < 2000$ . From Fig. 7, we see that our limits translate into an upper bound on  $\Delta z/z_{1/2}$  of  $\Delta z/z_{1/2} < 0.5$ .

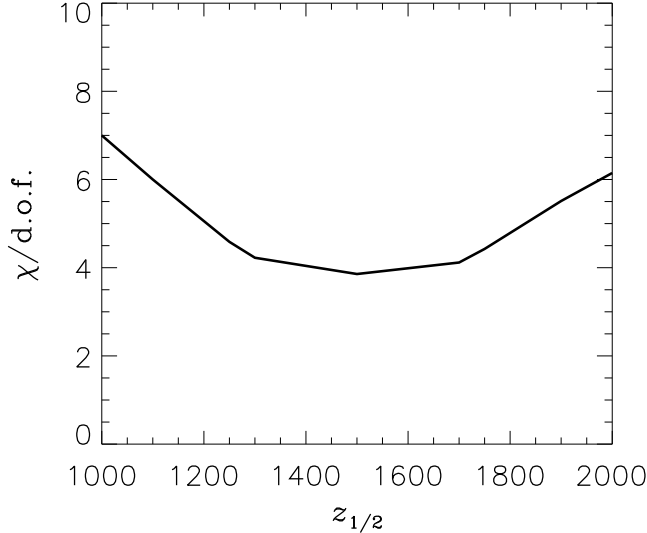


FIG. 8. The  $\chi^2$  for the case of  $\Delta z = 0$  as a function of  $z_{1/2}$ .

### III. CONCLUSIONS

Our investigation of the effect of a non-standard ionization history on the CMB using a change in the overall ionization/recombination rates (through the parameter  $a$ ) and in the binding energies (through the parameter  $b$ ) appears to provide a very general framework for studying such variations in the standard model. In particular, it seems possible to model arbitrary changes in both the epoch of last scattering and in the width of the last-scattering surface through such variations, with the exception of ionization histories having a narrow, high-redshift surface of last scattering, for which the ionization fraction decreases faster than in the equilibrium case.

Our results indicate that the BOOMERANG and MAXIMA results with  $\Omega_b h^2 = 0.019$  (from BBN) can be well-fit over a broad range of choices for  $a$  and  $b$ . However, the lower bounds on  $a$  and  $b$  are quite robust (i.e., nearly independent of variation in the other parameter). We find that  $b > 0.5$  and  $\log(a) > -1.6$  at the 95% confidence level. If we restrict  $a$  to its standard model value, changing only the binding energies, the allowed (95%) region is given by  $0.5 < b < 1.1$ . Similarly, if we restrict the binding energies to be unchanged ( $b = 1$ ) and change only the overall rates, then  $a$  is constrained to lie in the range  $-1.6 < \log(a) < 0.4$ .

One robust prediction of all of these models is a decrease in the amplitude of the third peak, relative to its height in the standard model. We have scanned over our allowed region in Fig. 1 and found that this result is independent of the particular values of  $a$  and  $b$ . In Table I we show results for different pairs of  $a, b$  within the allowed region. The last entry is the best fit standard model with high baryon density. This model predicts a much higher third peak (smaller  $X$ ) than the other models.

Our results are more general than previous comments that models with late recombination can be distinguished from high  $\Omega_b h^2$  models by the amplitude of the third peak. Our allowed region includes models with recombination at slightly *higher* redshift than in the standard model (including the model in Table I with  $a = 0.03$  and  $b = 1.25$ ). For these models, the third peak is still reduced in amplitude, but this reduction is due to diffusion damping from an increase in the width of the surface of last scattering, rather than from a decrease in the redshift of last scattering as in Refs. [9] - [15]. Our results seem to imply that any modification in the recombination history which fits the BOOMERANG and MAXIMA observations will result generically in a decrease in the height of the third peak.

However, we also find that the actual height of the third peak is a function of  $a$  and  $b$ . From Table I it can be seen that this ratio increases as we move through the allowed region from small  $a$ , large  $b$  to large  $a$ , small  $b$ . So if the universe did have a non-standard ionization history, the amplitude of the third peak should allow us to determine precisely the nature of the deviation of  $x_e(z)$  from its standard evolution.

We thank U. Seljak and M. Zaldariagga for the use of CMBFAST [19]. R.J.S. was supported in part by the DOE (DE-FG02-91ER40690).



- 
- [1] P. de Bernardis et al., *Nature* **404**, 995 (2000).
  - [2] S. Hanany et al., *Astrophys. J. Lett.*, submitted, astro-ph/0005123.
  - [3] M. White, D. Scott, & E. Pierpaoli, *Astrophys. J.*, in press, astro-ph/0004385.
  - [4] A.E. Lange, et al., *Phys. Rev. D*, submitted, astro-ph/0005004.
  - [5] A.H. Jaffe, et al, astro-ph/0007333.
  - [6] M. Tegmark, M. Zaldarriaga, and A.J.S. Hamilton, astro-ph/0008167.
  - [7] K.A. Olive, G. Steigman, and T.P. Walker, *Phys. Rep.* **333**, 389 (2000).
  - [8] S. Burles, K.M. Nollett, and M.S. Turner, astro-ph/0008495.
  - [9] P.J.E. Peebles, S. Seager, & W. Hu, astro-ph/0004389.
  - [10] S. Hannestad, *Phys. Rev. D*, **60**, 023515 (1999).
  - [11] M. Kaplinghat, R.J. Scherrer, and M.S. Turner, **60**, 023516 (1999).
  - [12] M. Tegmark, A. Taylor and A. F. Heavens, *Astrophys. J.* **479**, 568 (1997).
  - [13] R.A. Battye, R. Crittenden, and J. Weller, astro-ph/0008265.
  - [14] P.P. Avelino, C.J.A.P. Martins, G. Rocha, and P. Viana, astro-ph/0008446.
  - [15] S.L. Landau, D.D. Harari, M. Zaldarriaga, astro-ph/0010415.
  - [16] P. J. E. Peebles, *Astrophys. J.* **153**, 1 (1968).
  - [17] B. J. T. Jones & R. F. G. Wyse, *A&A* **149**, 144 (1985).
  - [18] L. Spitzer & J. L. Greenstein, *Astrophys. J.* **114**, 407 (1951).
  - [19] U. Seljak and M. Zaldarriaga, *Astrophys. J.* **469**, 437 (1996).

TABLE I. The height of the first peak relative to the height of the third peak,  $X \equiv C_l(\text{1st peak})/C_l(\text{3rd peak})$ , for different models.

$a$	$b$	$\Omega_b h^2$	$X$
0.03	1.25	0.019	6.24
0.1	1.0	0.019	3.72
1.0	0.75	0.019	3.02
10.0	0.65	0.019	2.82
1.0	1.0	0.030	1.84